

Towards single particle imaging of human chromosomes at SACLA

This content has been downloaded from IOPscience. Please scroll down to see the full text.

2015 J. Phys. B: At. Mol. Opt. Phys. 48 244007

(<http://iopscience.iop.org/0953-4075/48/24/244007>)

View [the table of contents for this issue](#), or go to the [journal homepage](#) for more

Download details:

IP Address: 128.41.35.28

This content was downloaded on 04/04/2016 at 13:20

Please note that [terms and conditions apply](#).

Towards single particle imaging of human chromosomes at SACLA

Ian Robinson^{1,2,3}, Joerg Schwenke^{1,2}, Mohammed Yusuf^{1,2},
Ana Estandarte^{1,2}, Fucui Zhang^{1,2}, Bo Chen^{1,2,3}, Jesse Clark^{4,5},
Changyong Song⁶, Daewoong Nam⁶, Yasumasa Joti^{7,8}, Kensuke Tono^{7,8},
Makina Yabashi^{7,8}, Gina Ratnasari⁹, Kohei Kaneyoshi⁹,
Hideaki Takata⁹ and Kiichi Fukui⁹

¹London Centre for Nanotechnology, University College, Gower St, London, WC1E 6BT, UK

²Research Complex at Harwell, Rutherford Appleton Laboratory, Didcot, OX11 0FA, UK

³School of Materials Science and Engineering, Tongji University, Shanghai, People's Republic of China

⁴Stanford PULSE Institute, SLAC National Accelerator Laboratory, Menlo Park, CA 94025, USA

⁵Center for Free-Electron Laser Science (CFEL), Deutsches Elektronen Synchrotron (DESY), Notkestrasse 85, D-22607 Hamburg, Germany

⁶Pohang University of Science and Technology, 77 Cheongam-ro, Nam-gu, Pohang-si, Gyeongsangbuk-do, Korea

⁷Japan Synchrotron Radiation Research Institute, 1-1-1 Kouto, Sayo, Hyogo Prefecture 679-5198, Japan

⁸RIKEN SPring-8 Center, 1-1-1 Kouto, Sayo, Hyogo Prefecture 679-5148, Japan

⁹Osaka University, 2-1 Yamadaoka, Suita 565-0871 Osaka, Japan

E-mail: i.robinson@ucl.ac.uk

Received 16 July 2015, revised 6 October 2015

Accepted for publication 14 October 2015

Published 3 November 2015



CrossMark

Abstract

Single particle imaging (SPI) is one of the front-page opportunities which were used to motivate the construction of the first x-ray free electron lasers (XFELs). SPI's big advantage is that it avoids radiation damage to biological samples because the diffraction takes place in femtosecond single shots before any atomic motion can take place in the sample, hence before the onset of radiation damage. This is the 'diffract before destruction' theme, destruction being assured from the high x-ray doses used. This article reports our collaboration's first attempt at SPI using the SACLA XFEL facility in June 2015. The report is limited to experience with the instrumentation and examples of data because we have not yet had time to invert them to images.


Keywords: chromosome, radiation damage, diffraction, metaphase, iterative phasing, coherence, imaging

(Some figures may appear in colour only in the online journal)

Introduction

There are two proposed methods of presenting samples to the x-ray free electron laser (XFEL) beam for single particle imaging (SPI): particle injection and membrane-scanned samples. Particle-injection SPI was the main design goal of the CXI instrument at Stanford's LCLS project, but this

beamline has evolved into a 'serial femtosecond crystallography' facility and its SPI capabilities have not been so strongly developed. SPI was also an early application of the AMO beamline of LCLS using the user provided CAMP chamber. Virus structure was an early promise of SPI because the high symmetry of some viruses could be used to obtain multiple views of a sample and achieve single-shot 3D imaging. This is the same idea as 'non-crystallographic symmetry'. For signal reasons, it was found that very large viruses were needed for the experiment to work well. Impressive 3D images of a mimi-virus, obtained by the Hajdu group, show

 Content from this work may be used under the terms of the [Creative Commons Attribution 3.0 licence](https://creativecommons.org/licenses/by/3.0/). Any further distribution of this work must maintain attribution to the author(s) and the title of the work, journal citation and DOI.

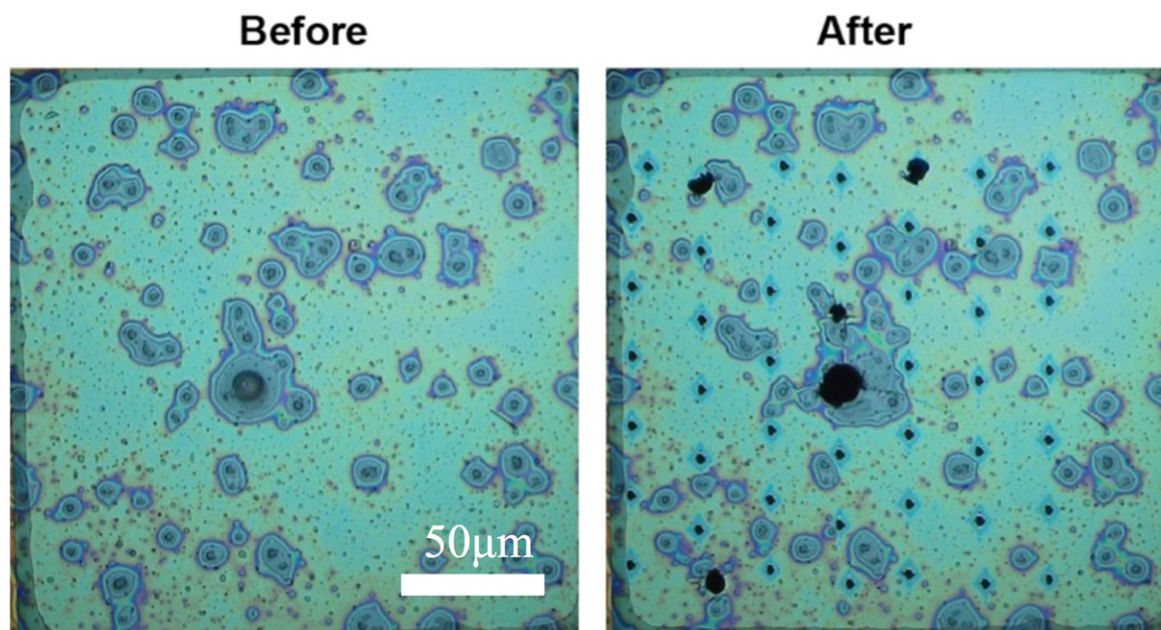


Figure 1. Optical microscope image of a $200 \times 200 \mu\text{m}$ Silicon Nitride (SiN) membrane, 150 nm thick, coated with a small density of human HeLa S3 chromosomes. The sample was prepared with a non-aqueous ionic liquid which survives insertion into vacuum. Left: before irradiation. Right: after irradiation with a 7×7 array of XFEL shots, spaced $25 \mu\text{m}$ apart.

significant internal structure [1, 2]. Another important direction is ‘Live cell imaging’ with single XFEL shots applied to previously living cells in a thin liquid environment. *Microbacterium lacticum* cells were sandwiched between two SiN membranes and imaged with single XFEL shots in an impressive demonstration of this application [3]. Live cyanobacteria [4] have also been imaged using the liquid jet XFEL method. Cyanobacteria had been previously imaged in a sandwich-type cell by synchrotron-based CDI [5] although the feasibility of achieving the apparent 50 nm resolution in wet cells with non-XFEL beams has been questioned [6].

Carboxysomes are polyhedral particles involved with the fixation of CO_2 in cyanobacteria. They appear icosahedral in the electron microscope with sizes from 90–500 nm. They are difficult to crystallize because of this size variation. The particles contain a large number of ribulose biphosphate carboxylase/oxygenase (Rubisco) clusters (11 nm diam), sometimes forming internal arrays. Rubisco is the most common protein on our planet and is vital to life. Hantke *et al* imaged carboxysome particles by injecting them into the CXI station at LCLS [7]. The individual images avoided the size dispersity problem, but clearly showed their icosahedral symmetry. This work demonstrated the utility of non-damaging x-ray imaging filling the gap between optical and electron microscopy resolutions.

The particle injection method is very wasteful of material, with gram quantities of protein sometimes needed for a run of a few hours, collecting diffraction patterns at 120 Hz at LCLS. Less than 1 in 10^9 particles typically gets hit directly. Technical improvements such as using a lipidic-phase propellant have improved this situation [8], but are not always compatible with the samples.

An alternative method was developed by the group of Changyong Song at the Spring-8 angstrom compact free electron laser (SACLA) XFEL facility [9], adjacent to the Spring8 synchrotron facility in Japan. The MAXIC chamber [10] uses a fast-scanning mechanical raster system to move membrane samples through the beam at up to 30 Hz repetition rate. The scanner is fast enough to separate each shot beyond the circle of debris (Figure 1), but some seconds are wasted moving from one membrane window to the next. Imaging of the mammalian nucleus has been achieved in this way [11]. In the work reported here, because of the difficulty of handling whole chromosome samples, we used the membrane-scanning, rather than particle-injection, method to measure human chromosomes with single shots of x-rays from SACLA in order to obtain damage-free images.

Methods

A b-lymphobalstoid male Yoruba cell line (passage 4) was grown at 37°C in a 5% CO_2 atmosphere in RPMI medium (Sigma, UK) supplemented with penicillin/streptomycin (Sigma, UK) and 20% fetal bovine serum (FBS) (Sigma, UK). Mitotic cells were enriched using a thymidine block with the addition of 2 mM thymidine for 16 h and then arresting the mitotic cells after treating the cells with colcemid $0.2 \mu\text{g ml}^{-1}$ (Gibco Life Technologies, UK) for 16 h. Polyamine mitotic chromosomes were prepared by treatment with a prewarmed hypotonic, 0.075 M KCl (VWR BDH Prolabo, UK) for 15 min and then resuspended into polyamine buffer [12, 13] or in methanol acetic acid [14].

Chromosomes were prepared for x-ray imaging according to a previously published protocol [15, 16]. The

chromosome sample was fixed in glutaraldehyde and placed onto a silicon nitride window containing $150\ \mu\text{M}$ of SYBR gold stain. The sample was washed in water to remove residues of dye. Chromosome preparations were verified by imaging using a Zeiss AxioZ2 fluorescence microscope with ISIS software or an Olympus LEXT-OLS4000. For some of the membranes, chromosomes were stained with platinum blue [14], at a concentration 5 mM for 30 min and washed for 5, 10, and 15 min in water. Chromosome samples were either dehydrated using an ethanol series and left to air dry or were dried using hexamethyldisilazane.

A parallel set of samples was prepared using HeLa S3 human cervical cancer cell line. HeLa S3 cell was cultured at $37\ ^\circ\text{C}$ in a 5% CO_2 atmosphere in RPMI 1640 medium (Nacalai Tesque, Japan) with 5% of FBS. To obtain mitotic cells, colcemid was added (final concentration $0.1\ \mu\text{g ml}^{-1}$) 16 h before harvesting. Mitotic chromosomes were isolated by polyamine method [17] and applied onto 0.01% poly-L-lysine coated silicon nitride windows, kept on ice for 10 min. After incubation in XBEO buffer (10 mM HEPES, pH 7.7, 100 mM KCl and 5 mM EGTA) for 30 min, the chromosomes were fixed with 2.5% glutaraldehyde/XBEO for 30 min. After washing with XBEO three times for 5 min each, a solution of 0.5% ionic liquid, 1-butyl-3-methylimidazolium tetrafluoroborate (BMI-BF₄, Merck), was applied onto the samples for 1 min incubation [18]. Afterwards, extra ionic liquid was removed by filter paper, and the chromosome samples were air dried.

The 36×36 window membrane arrays used by MAXIC were screened under an optical microscope to draft maps of the densely covered regions, which were then entered into the LabView interface of the MAXIC chamber. We scanned a total of 20 membrane arrays in five batches of 4. Measurements were made at BL3 of the SACLA facility [19]. With 1 h downtime between batches for breaking vacuum, our collaboration's 48 h run in June 2015 resulted in 400 000 exposures (12 TB) of diffraction data. Some membranes were found not to diffract and were skipped by observant operators. SACLA ran very well during the entire beamtime with very few interruptions. We used 4 keV x-rays at 10 Hz to have a strong signal from biological samples $1\ \mu\text{m}$ thick. The multiport charge-coupled device (MPCCD) detector [20] worked well and gave data with low background.

The first 3 h were used for beamline alignment and testing the effect of closing the Kirkpatrick–Baez (KB) mirror entrance slits located 4 m in front of the sample chamber in order to enlarge the focus size. The KB focussing system produced a focus of $1.5\ \mu\text{m}$, which is smaller than some of the chromosomes we wanted to study. Diffraction-limit effects at the slit allow the focus to be enlarged to match the size of the samples, several microns in some cases, and still stay within the oversampling range of the detector ($50\ \mu\text{m}$ pixels at 1.5 m). When the slit size was $1 \times 1\ \text{mm}$, the focus was measured to be $1.7\ \mu\text{m} \times 1.4\ \mu\text{m}$ with a wire scan. When the slits were closed to $0.25 \times 0.25\ \text{mm}$ we found it gave $2.1\ \mu\text{m}$, 0.1×0.1 gave $3.6\ \mu\text{m}$, 0.06×0.06 gave $4.3\ \mu\text{m}$ and 0.04×0.04 gave $5.9\ \mu\text{m}$, all in the vertical direction. In order

not to lose too much flux, we decided on $0.25 \times 0.25\ \text{mm}$ slits about 6 h into the run.

Results

As can be seen in figure 1, the sample we prepared contains only chromosome suspension, with almost no nucleus or chromosome cluster material. Almost all the chromosomes were individually suspended in the buffer solution and have been scattered on the substrate surface following sample preparation. The sizes of the isolated chromosomes ranged from 1 to $3\ \mu\text{m}$.

Initially we were concerned about breaking membranes with the beam. Most exposed 100 nm thick windows were found to have burst after seeing the full beam. This could have been partly due to the vacuum shock, since there were still diffraction patterns seen in some cases. But after closing the slits, the problem of burst windows was reduced to a rare event. 150 and 200 nm thick windows survived without breakage. In figure 1 we observed that the extent of the damage caused by the beam depends on the size of the object that was hit—big objects lead to bigger holes, presumably because more energy is absorbed. Cracks can be observed around the biggest hole.

The damage surrounding each XFEL shot can be seen in the images of figure 1. Empty regions of the membrane show a circle of visible alteration about $5\ \mu\text{m}$ in diameter. Places where the ionic liquid pools are visualized by their Newton rings remain unchanged outside this diameter. The drilled holes appear to be about $3\ \mu\text{m}$ in diameter, not far from the size measured with wire scans. Three locations originally containing small objects, about the size of single chromosomes, give rise to holes (dark circles) about $5\ \mu\text{m}$ in diameter. The one direct hit on a large object, $10\ \mu\text{m}$ in diameter, probably an unburst cell nucleus, produced a hole about $13\ \mu\text{m}$ in diameter and the appearance of cracks in the membrane.

A very rough scaling relation can be inferred from these observations. A cell nucleus contains a mass at least 46 times bigger than a single chromosome and shows a damage circle diameter, $d = 2.6$ times bigger. We can understand this behavior in terms of the two-dimensional heat diffusion equation applied to heat flow within the membrane,

$$\frac{\partial T}{\partial t} = D \left(\frac{\partial^2 T}{\partial x^2} + \frac{\partial^2 T}{\partial y^2} \right),$$

where the symbol D represents the ratio of the thermal conductivity to the density per unit area of the membrane material. Following an impulse of heat at the origin, Q_0 , the temperature follows a time-dependent Gaussian distribution,

$$T(x, y, t) = \frac{Q_0}{4\pi Dt} e^{-(x^2+y^2)/4Dt}.$$

This will reach the melting point of the membrane everywhere within a circle of diameter d , where it can be

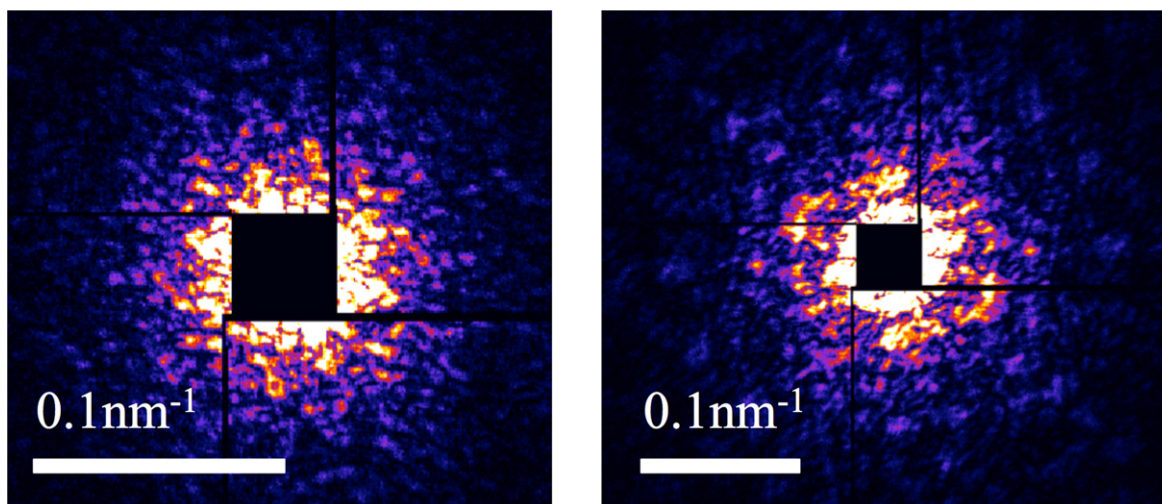


Figure 2. Examples of XFEL SPI diffraction data collected from human chromosome samples mounted on SiN membranes. The central square is the gap between the panels of the MPCCD detector, which is 60×60 pixels wide. Good 2-fold symmetry of the patterns can be seen.

shown that d scales with the square root of the heat input Q_0 . We consider that the holes punctured in the membrane of figure 1 are melted by the heat of x-ray absorption in the mass of sample in the beam. We can therefore deduce that in our experiment, the nucleus in figure 1 received $(2.6)^2 = 7$ times the amount of heat input from the x-ray beam as the single chromosomes. This seems reasonable considering that the beam size of $2.1 \mu\text{m}$ falls well within the $10 \mu\text{m}$ nuclear diameter, so only about 7 of its 46 chromosomes would have been actually hit by the beam. There are large uncertainties in these estimates, of course, coming from a variety of assumptions.

A large number of diffraction patterns was collected during the experiment running at 10 Hz for most of the 48 h run. The hit rate varied considerably from sample to sample. We used the ‘RunDataViewer’ ImageJ plug in to view the 49 diffraction patterns from each membrane in turn [21]. Typically there were about 3 hits per membrane. We manually selected diffraction patterns for inversion into images. The size of the objects recorded was also found to vary. Sometimes only the central maximum of the diffraction pattern was lost in the 60×60 pixel central hole of the MPCCD detector. This corresponds to diffraction from an object 280 nm in size. However on other examples as shown in figure 2, the speckles were about 15 pixels across, from objects around 560 nm across. The diffraction intensity can be seen to extend to around 0.06 nm^{-1} , suggesting that images with 100 nm resolution might be expected. Also, these examples have several fringes of missing data due to the central hole, which we expect will challenge the reconstruction algorithms [22].

Discussion

The central hole in the MPCCD detector [20] is an unavoidable consequence of the forward scattering geometry.

The four central detector panels were adjusted carefully at the start of the experiment to get as close as possible to the direct beam without saturating the closest pixels. Nevertheless, this leads to missing 60×60 pixels in the center of the diffraction patterns. A second MPCCD detector was positioned at 3.0 m from the sample behind the missing hole, but this was also protected by a beam stop which blocked most of the data recorded there.

While we expect to obtain good images from the diffraction patterns despite the missing data [20], there are potential improvements to the measuring system that could be implemented. Recording the direct beam behind an attenuator of the second detector could work. This would allow filling in of the missing region after scaling and adjustment. In our experience, in previous CDI and ptychography experiments performed elsewhere, this has not worked as well as we would have liked.

Instead, it might be interesting to consider putting an in-line holography setup inside the central hole instead of the second diffraction detector (which was mostly covered by a beam stop). We are developing a modulator-based single-shot imaging system (called coherent modulation imaging—CMI), which could be employed here [23]. Getting a real space image would allow the synthesis of the missing diffraction data on the first detector.

Acknowledgments

This work was partially funded by the UK Biotechnology and Biological Sciences Research Council (BBSRC) and Engineering and Physical Sciences Research Council (EPSRC). JC was supported by a fellowship from the Volkswagen Stiftung. The experiments were performed at BL3 of SACL A with the approval of the Japan Synchrotron Radiation Research Institute (JASRI) under Proposal No. 2015A8029.

References

- [1] Marvin Seibert M *et al* 2011 Single mimivirus particles intercepted and imaged with an x-ray laser *Nature* **470** 78
- [2] Ekeberg T *et al* 2015 Three-dimensional reconstruction of the giant mimivirus particle with an x-ray free-electron laser *Phys. Rev. Lett.* **114** 098102
- [3] Kimura T *et al* 2014 Imaging live cell in micro-liquid enclosure by x-ray laser diffraction *Nat. Commun.* **5** 3502
- [4] van der Schot G *et al* 2015 Imaging single cells in a beam of live cyanobacteria with an x-ray laser *Nat. Commun.* **6** 5704
- [5] Nam D *et al* 2013 Imaging fully hydrated whole cells by coherent x-ray diffraction microscopy *Phys. Rev. Lett.* **110** 098103
- [6] Bartels M, Krenkel M, Haber J, Wilke R N and Salditt T 2015 X-ray holographic imaging of hydrated biological cells in solution *Phys. Rev. Lett.* **114** 048103
- [7] Hantke M F *et al* (Hajdu Group) 2014 High-throughput imaging of heterogeneous cell organelles with an x-ray laser *Nat. Photonics* **8** 943–9
- [8] Johansson L C *et al* 2012 Lipidic phase membrane protein serial femtosecond crystallography *Nat. Methods* **9** 263
- [9] Ishikawa T *et al* 2012 A compact x-ray free-electron laser emitting in the sub-angstrom region *Nat. Photonics* **6** 540
- [10] Song C *et al* 2014 Multiple application x-ray imaging chamber for single-shot diffraction experiments with femtosecond x-ray laser pulses *J. Appl. Cryst.* **47** 188
- [11] Song C, Takagi M, Park J, Xu R, Gallagher-Jones M, Imamoto N and Ishikawa T 2014 Analytic 3D imaging of mammalian nucleus at nanoscale using coherent x-rays and optical fluorescence microscopy *Biophys. J.* **107** 1074–81
- [12] Yusuf M, Parmar N, Bhella G K and Robinson I K 2014 A simple filtration technique for obtaining purified human chromosomes in suspension *BioTechniques* **1** 257
- [13] Yusuf M, Chen B, Hashimoto T, Estandarte A K, Thompson G E and Robinson I K 2014 Staining and embedding of human chromosomes for 3D serial block face scanning electron microscopy *BioTechniques* **1** 302
- [14] Shemilt L A, Estandarte A K C, Yusuf M and Robinson I K 2014 Scanning electron microscope studies of human metaphase chromosomes *Phil. Trans. R. Soc. A* **372** 20130144
- [15] Nishino Y, Takahashi Y, Imamoto N, Ishikawa T and Maeshima K 2009 Three-dimensional visualization of a human chromosome using coherent x-ray diffraction *Phys. Rev. Lett.* **102** 18101
- [16] Shemilt L, Verbanis E, Schwenke J, Estandarte A K, Xiong G, Harder R, Parmar N, Yusuf M, Zhang F and Robinson I K 2015 Karyotyping human chromosomes by optical and x-ray ptychography methods *Biophys. J.* **108** 706
- [17] Hayashihara K, Uchiyama S, Kobayashi S, Yanagisawa M, Matsunaga S and Fukui K 2008 Isolation method for human metaphase chromosomes *Protoc. Exch.* doi:10.1038/nprot.2008.166
- [18] Dwiranti A, Lin L, Mochizuki E, Kuwabata S, Takaoka A, Uchiyama S and Fukui K 2012 Chromosome observation by scanning electron microscopy using ionic liquid *Microsc. Res. Tech.* **75** 1113
- [19] Tono K *et al* 2013 Beamline, experimental stations and photon beam diagnostics for the hard x-ray free electron laser of SACLA *New J. Phys.* **15** 083035
- [20] Kameshima T *et al* 2014 Development of an x-ray pixel detector with multi-port charge-coupled device for x-ray free-electron laser experiments *Rev. Sci. Instrum.* **85** 033110
- [21] Joti Y *et al* 2015 Data acquisition system for x-ray free-electron laser experiments at SACLA *J. Synchrotron Radiat.* **22** 571
- [22] Huang X *et al* 2009 Soft x-ray diffraction microscopy of a frozen hydrated yeast cell *Phys. Rev. Lett.* **103** 198101
- [23] Zhang F, Chen B, Morrison G R, Guizar-Sicairos M and Robinson I K 2015 X-ray coherent modulation imaging *Nat. Photonics* submitted